

Stable Walking on Variable Visco-Elastic Terrains using Meta-parameters for Passive State Migration

Valerio Pereno, Kya Shoar, Giulia Bartoli, Fabio Bianchi and Thrishantha Nanayakkara

Abstract—This paper investigates how a walker could estimate the variability of an arbitrary set of state variables when migrating on visco-elastic grounds. The state variables are a function of both the visco-elastic settings of the walking body and soft terrain parameters. A rimless wheel model was developed using a Lagrangian approach in order to obtain analytical solutions for migration across ground conditions. An algorithm was then developed to determine the steady value of the variables as a function of the difference in ground and hub parameters involved in the migration. A generalised migration metaparameter, Δ_g , function of this difference, was then extrapolated using polynomial approximation. Δ_g can be used to estimate the expected variability at a state given information on actual and previous ground parameters. A second parameter, Δ_h , describing local variability of a given state on a given terrain, is used to generate a predictive algorithm capable of stabilising the rimless wheel setup when subject to an abrupt change in ground parameters. We actuate the rimless wheel with a constant torque leaving it to develop any speed profile for a given visco-elastic impedance distribution of the ground and its own vertical visco-elastic impedance. The ground is altered depending on the two migration meta-parameters (Δ_g and Δ_r), ensuring both local and migration stability.

I. INTRODUCTION

When a skier walks from a snowy terrain to the floor of a mountain chalet with his boots on, he/she would change his/her muscle tension to maintain the variability of state variables within safe margins to avoid slipping and falling. Depending on the softness of the snow and the style of the chalet's floor, the skier would have to implement less or more rigid control strategies in order to achieve desired variability margins. This suggests an adaptive internal control strategy to change the visco-elastic parameters of the limb joints to suit those of the terrain. A suggested method to recreate such adaptation is Impedance Control Theory, which has been used in many fields, such as robotic excavation [1], automated massage systems [2], safe interaction with human companions [3], rehabilitation [4], prosthetics [5], exoskeletons [6], and biped locomotion [7] etc. Impedance Control Theory [8]-[10] proposes that a body in dynamic contact with the environment should be able to adapt its internal impedance (stiffness, damping, and inertia gains) in order to maintain a stable dynamic coupling with the environment, a concept directly applicable in bipedal robotic

locomotion. Another approach is to estimate the impedance parameters of the environment to tune the internal parameters of the manipulator as proposed in disturbance observers [11] and linear estimation of environment's impedance parameters [2],[12]. Both cases have been applied in [13] to passive-dynamic locomotion, and it has been shown how artificially varying impedance parameters in a joint can help control the variability of collision force at the contact point between ground and walker.

When a giraffe calf is born, it will at first struggle to stay upright, and it will fall numerous times when attempting to walk. After a few hours, the calf will however be able to walk stably, and as time passes it will refine its ability to interact with the environment for more complex motion. Despite the required learning curve, this behaviour suggests that the newborn cub has some kind of memory imprinting, or primitive, which allows it control over its limbs to initialise walking motion. The existence of such memory primitives relating to locomotion has been theorized in animals and humans alike [14]. Memory primitives are a set of internal data sets, representing joint parameters, which can be visualised as state-space representations of contact forces, which are subconsciously scanned for the optimal internal settings to match the kind of surface which is being walked on. The concept of memory primitives has been used in artificial intelligence systems many times before in [15], [16], albeit not in the field of robotic locomotion. As the cub grows, it will also encounter difficulties in the motion between different kind of surfaces, for example walking for the first time on sand. Through experience, the cub will be able to refine the memory primitives to achieve long-term stable locomotion [17].

Here we study how different sources of variability, mainly the ground configuration and the migration of the walker on the ground itself, affect stability in locomotion. Prior knowledge of the effect of variability can be used to find an alternative internal impedance control strategy to maintain the variability of walking within desired metastability bounds. Such study is carried out using simulations and tested experimentally by means of a rimless wheel. The rimless wheel represents the ideal form of underactuated modeling for bipedal locomotion, and has been used numerous times before for experimentation [18][19][20]. Inspiration for the proposed algorithm is taken from natural predisposition for adaptive locomotion, in the form of memory primitives. We present analytical results, numerical simulations, and experimental evidence of how it can passively migrate from one region in some arbitrary state space to another simply

*This work was partially supported by the Engineering and Physical Sciences Research Council, UK, under grant agreement EP/I028773/1.

Authors are with the Centre for Robotics Research (CoRe), Division of Informatics, King's College, London, WC2R 2LS, UK
valerio.pereno, kya.shoar, giulia.bartoli,
fabio.bianchi, thrish.antha at kcl.ac.uk

Special thanks to Jim Trotter, King's College London

by changing its internal impedance parameters, selecting the stable-most combination for the given surface of locomotion, and the stable-most path to a stable zone.

II. SOURCES OF VARIABILITY IN THE MOTION OF A COMPLIANT WALKER ON VISCO-ELASTIC TERRAIN

In the authors' previous work, it has been shown how it is possible to manipulate contact forces by altering internal impedance parameters to maintain stable coupling with an uncertain visco-elastic terrain [13]. However, it is not sufficient to just know the ideal internal visco-elastic parameters for achieving stability on a given surface. In [13], it has been found that the interaction effect between the coefficient of friction and the coefficient of restitution significantly affects the steady-state variability of a passive-dynamic walker. Since restitution and friction are indirectly related to the impedance parameters of the terrain and body, migration from one impedance context to another should account for the resulting change in the steady-state variability. Returning to the skier example, the variability, and therefore the control strategies implemented by the skier's brain, are related to the difference in ground conditions; i.e. the differences in stiffness and viscosity of the snow and of the chalet's floor. The magnitude and variability of state variables, for example the collision force, will depend greatly on the ground conditions of the departing state (the snow stiffness and viscosity) and will have an effect until the variables reach steady state condition. The memory primitive containing return force of collision between a foot and ground is visualised as a state-space landscape, varying in planar coordinates with internal impedance settings, and in height with the collision force as shown in Fig. 3. Migration from one point to another of this landscape will entail a variability landscape, as any ground condition can be paired with an 'ideal' internal setting, which minimizes collision force variability. Despite knowing this, previous work [13] shows that further sources of uncertainty must be present. Such variability generation has been identified in that arising when the walker migrates from one landscape to another, as the skier does in example cited above. This suggests that the contact force landscape for a certain ground condition will vary depending on which ground condition the walker originates from. The migration will bring the walker through a set of intermediate force landscapes, which will alter the stability.

In this paper, the authors have examined, both computationally and experimentally, the sources of variability pertaining to the migration of a walking machine from a ground surface to another, generalising an adaptation algorithm capable to stabilise the walker. In [21], the author uses Lyapunov functions to approximate regions of attraction around stable points for simple underactuated systems, thereby developing an algorithm capable of reaching any point of a bounded space with a probabilistic function representing the stability criterion for that point. [22] uses a complex modeling tool based on the receding horizon approach to stabilise steady-state trajectories. The model is based on the

solution of a jump-Riccati equation. Such equation will yield the minimum of the cost-to-go matrix, which represents the best migration pattern for the desired movement. However, solving the Riccati equations considerably increases the complexity of on-line calculations required to provide the necessary data to the feedback controller in order to compute settings that would allow the robot to achieve stability. Here, the authors propose to substitute the equations proposed in [22] with experimentally and computationally derived models, which are discretized and used to develop an internal algorithm ultimately capable of stabilizing a bipedal walker on uncertain and uneven terrain.

III. DYNAMICS OF A COMPLIANT WALKER WALKING ON A VISCO-ELASTIC TERRAIN

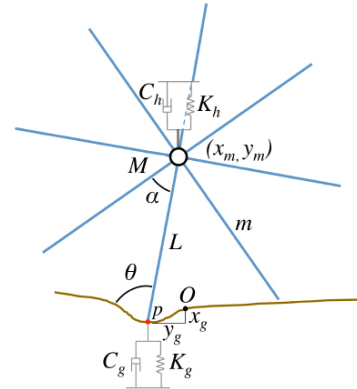


Fig. 1. Coupled system model of adaptive rimless wheel and visco-elastic ground.

Fig. 1 shows the main features of the experimental model. Mass-damper systems are used to model visco-elastic parameters of both ground and hub of the rimless wheel. For simplicity, the hub and the ground are restricted to move in the vertical direction only, which simplifies computation by restraining the simulation to the z-x plane. The vertical movement of both the hub and the ground are impeded by visco-elastic forces generated by two back-drivable motors. As shown in [13], the following equations are derived:

$$\dot{s} = \begin{bmatrix} \mathbf{0}_{3 \times 3} & \mathbf{0}_{3 \times 3} \\ \mathbf{I}_{3 \times 3} & \mathbf{0}_{3 \times 3} \end{bmatrix} s + \begin{bmatrix} A^{-1}u(s) \\ \mathbf{0}_{3 \times 1} \end{bmatrix} \quad (1)$$

IV. LOCAL VARIABILITY ANALYSIS

We first studied the limit cycle behavior of the nonlinear dynamics given in Equation 1 from [13] in order to understand how the internal impedance of the compliant walker affects the steady state variability of walking on an uncertain visco-elastic terrain. For a fixed ground condition, the hub parameters are altered in a sequential pattern in order to investigate the effect on stability criteria. Fig. 3 and 4 show the variable return map across collisions between the visco-elastic ground for 100 combinations of vertical stiffness and viscosity of the rimless wheel for a given distribution of the ground impedance $K_g = N(10, 1)$, $C_g = N(3, 0.3)$. The mesh shown indicates the average force (\bar{F}) and coefficient

of variation ($C_v = \frac{\sigma}{\bar{F}}$) of the return variable (in this case, normal force) at each point, computed from the numerous collisions for each point. The dots represent the single value of the variable at each collision. For each combination of hub impedance values, the system is re-initialized, so to exclude carried on variability and isolate local effects only. From the shape of such plots, it is possible to infer how, for the given ground distribution, there exist areas in the state-space where the variability is lower (i.e. the coefficient of variation of the collision forces is lowest). These points represent areas of stability, as low variability reduces the probability of an unpredictable perturbation in the return parameter, leading to instability. From the standard deviation mesh, a coefficient

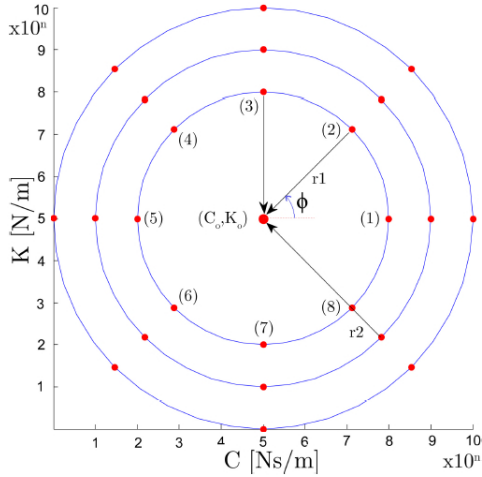


Fig. 2. Simulation setup, with variable radii of migration. N on the axis represents how internal parameters can be of any value.

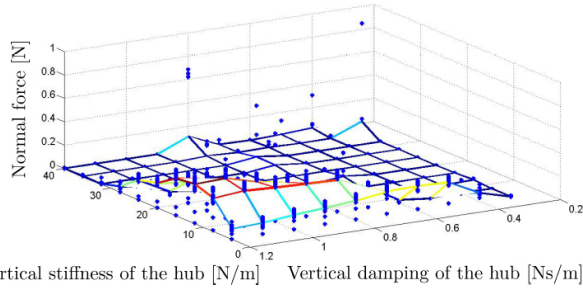


Fig. 3. Mean normal force for hub impedance combinations.

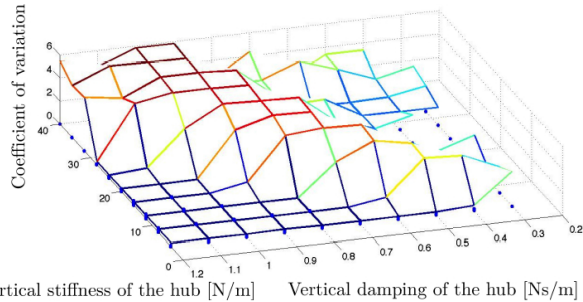


Fig. 4. Coefficient of variation for hub impedance combinations for a given ground.

of variation matrix is constructed:

$$C_v = \begin{bmatrix} C_{v[C_{h0}, K_{hN}]} & \cdots & C_{v[C_{hN}, K_{hN}]} \\ \vdots & \ddots & \vdots \\ C_{v[C_{h0}, K_{h0}]} & \cdots & C_{v[C_{hN}, K_{h0}]} \end{bmatrix} \quad (2)$$

where every entry of the matrix represents variability of collision forces at that combination of internal impedance parameters.

V. MIGRATION VARIABILITY ANALYSIS

The second source of variability examined relates to the variability that arises from the migration from one position in state-space to another. When a walker travels from a hard to a soft or more elastic terrain, he will carry over residual variability depending on the properties of the surface he is departing from. Furthermore, without any *a priori* knowledge of the future surface, the walker's internal settings will not adapt instantaneously. In [22], the authors use an on-line control system for stabilisation of non periodic trajectories of underactuated robots. Such an approach necessitates of thorough knowledge of the ground, derived from the receding-horizon model. In real-life, this is represented by a person walking blindfolded on uncertain ground. He will have no information about the ground until he has stepped on it. In this paper, in order to effectively compare and quantify the magnitude of migration along the state-space, common target conditions are defined. This method consists of constructing circles around an arbitrary centre point (C_o, K_o), as shown in Fig. 2. The distance of migration will then be determined by the radii of the circles. Firstly, the case where no migration occurs is considered, i.e. radius is equal to zero. This will be used as a benchmark, for comparison to the cases where migration occurs. Migrations will occur for a set number of points along each radius terminating at the centre point. Fig. 2 shows this migration, in the system parameter space. The circles are modeled using a standard circle function, where the radius is set from zero to the C (or K) coordinate of the system. Subsequently, the coefficient of variation ($C_v = \frac{\sigma}{\bar{F}}$) of the return force for the N points along the parameter is computed, together with the coefficient of variation at 0 (i.e. with no migration), and a variability index, δ , is defined as:

$$\delta_{C_v, n} = C_{v, n} - C_{v, 0}, \quad n = 1, 2, \dots, N \quad (3)$$

Where n is the position on the radius, as shown in Fig. 2. The variability index thus defined gives the difference between the coefficients of variance of the forces at each one of the eight points on the radius and the variability at the centre point. This will render explicit the effect of migrating from a condition inscribed on the radius to the centre point condition. By varying the position on the radius, a set of N variability indices are found for each radius, and the mean of the indices are computed for all the test radii:

$$\Delta_{C_v, r} = \bar{\delta}_{C_v, r} = \frac{1}{N} \sum_{n=1}^N \delta_{C_v, n}, \quad n = 1, 2, \dots, N \quad (4)$$

where r is the radius number. In this case, $N = 8$, hence eight points per radius are computed, as shown in Fig. 2. Therefore, for each migration radius, r , a parameter, $\Delta_{C_v, r}$ is defined. This analysis is carried out for both ground and hub migration. In the former, the hub is set to a fixed parameter, and the migration is carried out by the ground. Then, the hub parameters are changed, and the migration is repeated. This results in a set of Δ_g functions, as shown in 5. In the latter, the ground remain constant while the hub migrates across different conditions. Two parameters are hence derived, Δ_{r_g} and Δ_{r_h} .

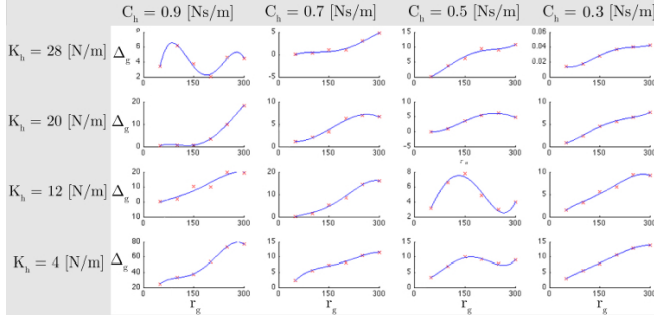


Fig. 5. Matrix of Δ_g functions (fitted polynomials in blue) for varying internal impedance combinations.

VI. ALGORITHM DEVELOPMENT

Having analyzed the results of the migration experiments, the following algorithm is proposed to control the adaptation of the rimless wheel. Firstly, the test shown in section V. is repeated for $N \times N$ combinations of hub K and C parameters, yielding Δ s as functions of r_g , as shown in equation 4. For each node in the matrix in Fig. 5, a function of Δ_g vs. r_g (where r_g is the magnitude of migration of the ground parameters) is produced, by generating coefficients of a fitted fourth order polynomial, as shown in Fig. 5. This will return a matrix containing four coefficients of the fitted polynomial for each subplot, which is the local memory primitive. These functions express the amount of variability induced on the walker due to the migration from previous ground conditions. This assumes that a walker, when departing a ground, has reached a steady-state stable combination of internal hub parameters, which will be conserved until collision with the following ground. To relate this to the skier example, this will give, for each internal parameter combination (representing the skier coming from any kind of possible ground) a variability due to the difference in conditions between the ground which is departed from, and the ground to which the walker moves. Therefore, the function of Δ_g can be computed for each point in the matrix shown in Fig. 5:

$$A_{f(r_g)} = \begin{bmatrix} \Delta_{f(r_g), [C_{h0}, K_{hN}]} & \cdots & \Delta_{f(r_g), [C_{hN}, K_{hN}]} \\ \vdots & \ddots & \vdots \\ \Delta_{f(r_g), [C_{h0}, K_{h0}]} & \cdots & \Delta_{f(r_g), [C_{hN}, K_{h0}]} \end{bmatrix} \quad (5)$$

It is assumed that the walker is provided with all current and future ground parameters. By substituting r_g into the

Δ_g function, a single value of Δ_{r_g} is found for each point:

$$A = \begin{bmatrix} \Delta_{r_g, [C_{h0}, K_{hN}]} & \cdots & \Delta_{r_g, [C_{hN}, K_{hN}]} \\ \vdots & \ddots & \vdots \\ \Delta_{r_g, [C_{h0}, K_{h0}]} & \cdots & \Delta_{r_g, [C_{hN}, K_{h0}]} \end{bmatrix} \quad (6)$$

This matrix is then multiplied elementwise with the return matrix derived in section IV, such that:

$$C_v^* = C_v \otimes A \quad (7)$$

This will return a new mesh-matrix, containing modified values of coefficient of variation, which is an adjusted memory primitive. Then, the minimum of this matrix is found. This minimum will correspond to a single K_h and C_h combination:

$$[K_h^*, C_h^*] = \min(C_v^*) \quad (8)$$

For this combination, a Δ_{r_h} function similar to that previously used is defined (from the process described in section V.) as a function of r_h which is the magnitude of the hub's migration (i.e. the magnitude of the parameter jump for the hub) to reach the stable point (i.e. K_h^* and C_h^* in equation

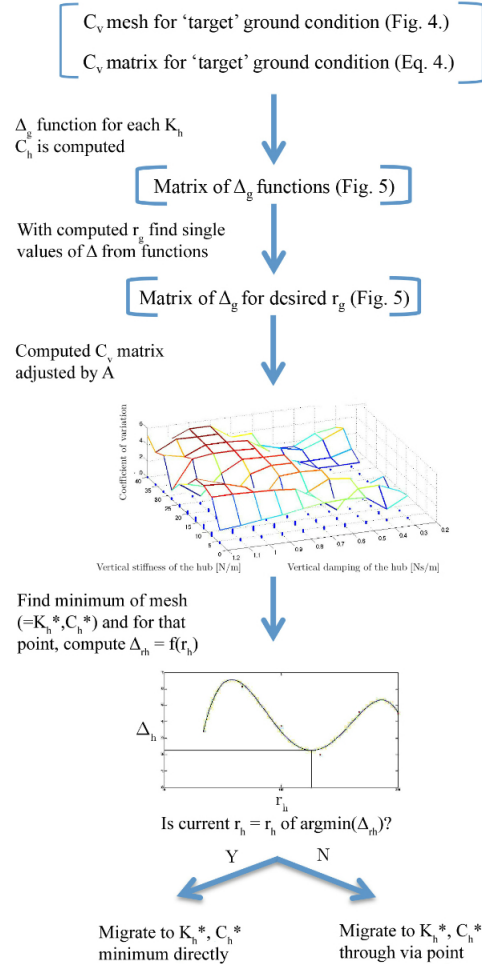


Fig. 6. Proposed algorithm, showing both local variability and migration variability.

8). Hence, the algorithm will check whether a point having a lower variability index Δ exists in the neighbourhood of the current point, by computing the minimum of the Δ_{r_h} function. If the value of r_h associated with the current hub configuration is not equal to that associated with the minimum found, then a path must be generated through a via point. This point will be any combination of K_h and C_h along the circle of the radius $r_{h_{min}}$ associated with the minimum of the Δ_h :

$$\sqrt{(K_h - K_{ho})^2 + (C_h - C_{ho})^2} = r_{h_{min}} \quad (9)$$

This ensures that the ultimate migration to the locally stable point is executed from the most migrationally stable hub configuration. This algorithm process is shown in Fig. 6.

VII. EXPERIMENTAL TESTING

The simulations were verified by means of experimental testing. The hardware arrangement is shown in Fig. 7. The rimless wheel was made of ABS plastic and driven by a motor (MAXON EC-max 30, 40W, geared at 1:81 gearing ratio) running in constant current mode at 396mA to render a torque $\tau = 0.05\text{Nm}$. The hub of radius 4.95cm weighed 0.65kg while each leg of length 6cm weighed 40g. The visco-elastic ground was constructed from an aluminum base connected through a rack and pinion setup to a MAXON EC-max 60, 400Watt, degeared motor. The pinion, of radius 4cm is used to minimize moment arm. The height of the central axis of the hub was also controlled using a position-derivative controlled back drivable servo motor (MAXON EC-max 40, 120 Watt, degeared) mounted in a rack and pinion arrangement to realize visco-elastic vertical impedance at the hub. In order to minimize the load on the motor, the rimless wheel was, furthermore, suspended by passive tension springs. Collision force was measured using an ATI technologies, Mini40 6-axis force/torque sensor at 100Hz sampling rate. The magnitude profile of the force vector was smoothed using a 3rd order Savitzky-Golay filter with a window size of 7. A peak detection algorithm was then used to extract peak collision forces.

Preliminary testing was carried out to test the validity of the setup, by experimentally reproducing the plot shown

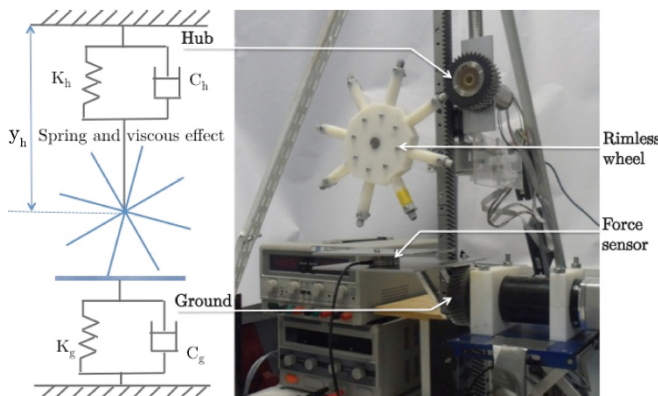


Fig. 7. Experimental setup and model.

in Fig. 8, and by carrying out the radius tests outlined in section V. After achieving satisfactory performance, the algorithm was tested. Fig. 8 shows the statistical analysis of the force data for the three cases: i. no internal adaptation, ii. adaptation without an algorithm, iii. adaptation with an algorithm. Each test was carried out for the same two ground conditions. It shows that for a sudden change in ground conditions and no internal adaptation the coefficient of variation noticeably increases. For hub adaptation with no algorithm, the hub reacts to ground changes by adjusting its internal values in order to migrate to a more stable region. Migrating through a via point decreases the coefficient of variation more significantly than migrating directly. Further investigation confirmed this trend for different ground conditions. The data therefore suggests that for the set of tested values stability is rather reached by adapting internal conditions through a via point. Using a two-sided T test it was verified that the force datasets collected for no adaptation of the hub statistically differed from both the case with and without the algorithm at the final stage. However, migrating through a via point does not guarantee a lower variability. It only does if the walker is not already at the minimum.

VIII. DISCUSSION

Exploitation of passive dynamics in underactuated walking has received increasing attention in the recent past [20], due to its efficiency and computational simplicity compared to that of rigid, fully actuated walkers. Study of a simple passive dynamic walker known as the rimless wheel [13], [15], [18] together with that of compass gait mechanisms in [23], [24], have been the most widely used methods of modeling passive dynamic legged locomotion. However, most previous work have been done on either deterministic ramps or stochastically rough terrain [18], [19]. In our previous work in [13], we showed how a passive dynamic walker can respond to changing ground impedance through adaptation of internal impedance to maintain limit-cycle stability. In [22], a solution is proposed for limit-cycle stability computation. However, the real-time computation of Riccati equations can be a daunting task in the case of changing ground impedance parameters. When a walker is in limit cycle stability on a given ground impedance, a sudden change in the ground impedance would cause the states to deviate to new regions of variability, causing unpredictable behavior. In such cases, an internal map relating the steady state variability of a given motion state such as the collision force, angular speed, etc., to the corresponding ground impedance and internal impedance of the walker, would provide a basis to develop an optimal predictive internal impedance control algorithm. However, memorizing all combinations of ground and internal impedance contexts would lead to a combinatorial explosion in search space. Here, we solve this problem by introducing two metaparameters, relating the change in force variability due to the magnitude of the change in impedance parameters for both terrain and system, which are used in a generic adaptive algorithm used to stabilize an experimental rimless wheel setup. The parameters are used to modify

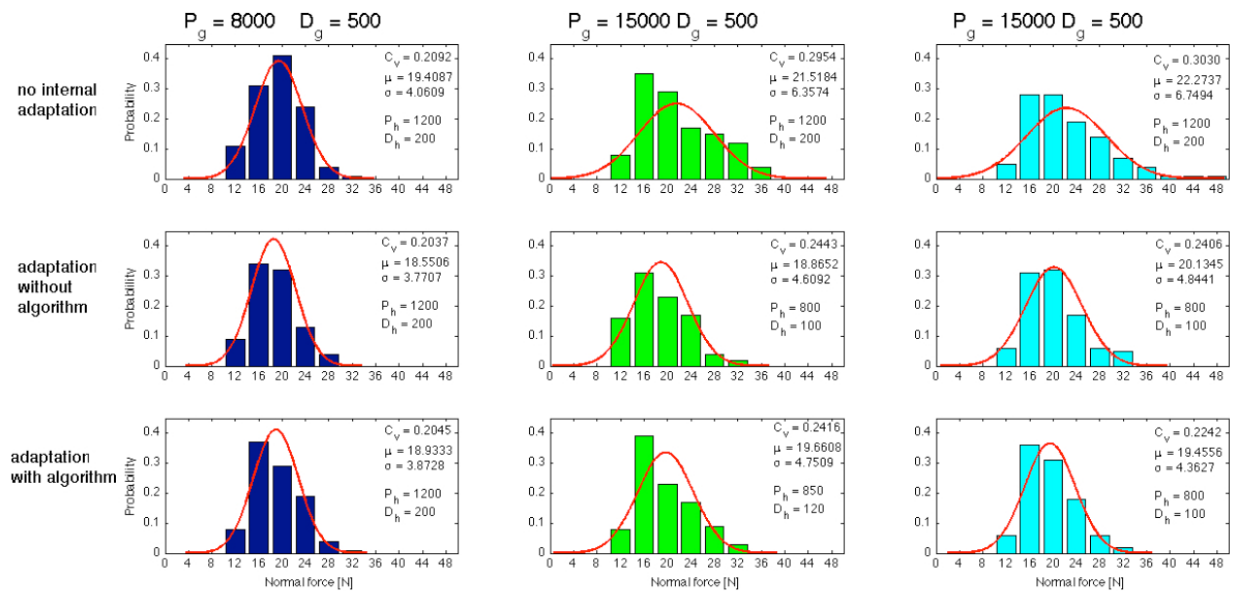


Fig. 8. Statistical analysis of the normal force data for three cases: i. no internal adaptation, ii. adaptation without an algorithm, iii. adaptation with an algorithm. The ground conditions are replicated for all three cases.

previously compiled local memory primitives. The proposed solution aims at investigating and predicting not only the local variability arising during walking, but an extended concept of variability, which is not solely dependent on the condition of the terrain, but considers previous conditions to compute an overall stability. This concept can be used to design efficient algorithms for dynamic walkers to passively migrate in a state space to maintain stability in the presence of ground impedance variability, reducing the computational burden to guarantee stability.

The algorithm proposed assumes perfect information of previous and future ground conditions. Future work must therefore focus on developing a framework to effectively sense ground parameters in real-time. A more autonomous adaptation to the environment can hence be achieved.

REFERENCES

- [1] S. Tafazoli, et al., "Impedance Control of a Teleoperated Excavator", *IEEE trans. on Control Systems Technology*, vol. 10, no. 3, 2002.
- [2] K. Mouri, et al., "Identification and Hybrid Impedance Control of Human Skin Muscle by Multi-Fingered Robot Hand", *In Proc. of the IEEE/RSJ IROS*, pp. 2895 - 2900, 2007.
- [3] A. De Luca, A. Albu-Schaeffer, S. Haddadin, G.Hirzinger, "Collision detection and safe reaction with the DLR-III lightweight manipulator arm" *IEEE/RSJ Int. Conference on Intelligent Robots and System*, Beijing, China, Oct 2006.
- [4] Y. Yang, L. Wang, J. Tong, and L. Zhang, "Arm Rehabilitation Robot Impedance Control ...", *in proc. of IEEE Int. Conf. on Rob. and Biomech.*, pp. 914 - 918, 2006.
- [5] J. W. Sensinger and R. F. Weir, "User-modulated impedance control of a prosthetic elbow in unconstrained, perturbed motion.", *IEEE trans. on Biomed. Eng.*, vol. 55, no. 3, 2008.
- [6] G. A. Ollinger, et al., "Active-Impedance Control of a Lower-Limb Assistive Exoskeleton", *in proc. of the IEEE 10th int. Conf. on Rhab. Robotics*, pp. 188 - 195, 2007.
- [7] H. O. Lim, et al., "Balance and Impedance Control for Biped Humanoid Robot Locomotion", *Procs. of IEEE/RSJ Int. Conf. on Intelligent Robots and Systems*, pp. 494 - 499, 2001.
- [8] N. Hogan, "Impedance Control: An Approach to Manipulation, Part I - Theory", *Journal of Dynamic Systems, Measurement, and Control*, vol. 107, pp. 1 - 7, 1985.
- [9] N. Hogan, "Impedance Control: An Approach to Manipulation, Part II - Implementation", *Journal of Dynamic Systems, Measurement, and Control*, vol. 107, pp. 8 - 16, 1985.
- [10] N. Hogan, "Impedance Control: An Approach to Manipulation, Part III - Applications", *Journal of Dynamic Systems, Measurement, and Control*, vol. 107, pp. 17 - 24, 1985.
- [11] R. J. Bickel and M. Tomizuka, "Disturbance Observer Based Hybrid Impedance Control", *In procs. of the American Control Conference*, pp. 729 - 733.
- [12] R. Kikuuwe and T. Yoshikawa, "Robot Perception of Environment Impedance", *Procs. of ICRA*, pp. 1661-1666, 2002.
- [13] Bianchi, Fabio, et al. "Adaptive internal impedance control for stable walking on uncertain visco-elastic terrains." *Intelligent Robots and Systems (IROS), 2012 IEEE/RSJ International Conference on. IEEE*, 2012.
- [14] Simion, Francesca, Lucia Regolin, and Hermann Bulf. "A predisposition for biological motion in the newborn baby." *Proceedings of the National Academy of Sciences* 105.2 (2008): 809-813.
- [15] Vaina, Lucia M., and Richard D. Greenblatt. "The Use of Thread Memory in Amnesic Aphasia and Concept Learning.(note 0)." (1979).
- [16] Tani, Jun, and Masato Ito. "Self-organization of behavioral primitives as multiple attractor dynamics: A robot experiment." *Systems, Man and Cybernetics, Part A: Systems and Humans, IEEE Transactions on* 33.4 (2003): 481-488.
- [17] Dominici, Nadia, et al. "Locomotor primitives in newborn babies and their development." *Science* 334.6058 (2011): 997-999.
- [18] T. Nanayakkara, K. Byl, H. Liu, X. Song, T. Villabona, "Dominant Sources of Variability in Passive Walking", *IEEE International Conference on Robotics and Automation (ICRA2012)*, RiverCentre, Saint Paul, Minnesota, USA, May 14-18, 2012, pp. 1003-1010.
- [19] K. Byl and R. Tedrake, "Metastable Walking on Stochastically Rough Terrain", *in Proceedings of Robotics: Science and Systems IV*, 2008 R. Inoue, F. Asano, D. Tanaka, and I. Tokuda, "Passive dynamic walking of combined rimless wheel and its speeding-up by adjustment of phase difference," *Proc. IROS*, pp. 2747 - 2752, 2011.
- [20] McGeer, Tad. "Passive dynamic walking." *The International Journal of Robotics Research* 9.2 (1990): 62-82.
- [21] Tedrake, Russ. "LQR-Trees: Feedback motion planning on sparse randomized trees." (2009).
- [22] Manchester, I. R., et al. "Stable dynamic walking over uneven terrain." *The International Journal of Robotics Research* 30.3 (2011): 265-279.
- [23] McGeer, Tad. "Passive walking with knees." *Robotics and Automation, 1990. Proceedings., 1990 IEEE International Conference on. IEEE*, 1990.
- [24] Van der Linde, R.Q. "Passive bipedal walking with phasic muscle contraction." *Biological cybernetics* 81.3 (1999): 227-237.